DESIGN, CALIBRATION AND TESTING OF TRANSIENT THIN FILM HEAT TRANSFER GAUGES

Kevin M. Kinnear†, and Frank K. Lu‡
NASA/UTA Center for Hypersonic Research
The University of Texas at Arlington
Arlington, TX 76019

ABSTRACT

A method for the design, construction, calibration and testing of thin film platinum resistance temperature detectors (RTDs) is described. The calibration and testing was performed to determine if RTDs can be used for measuring surface temperatures and heat transfer rates under transient conditions. By depositing a thin film of platinum on the surface of a highly polished ceramic substrate, RTDs were obtained which have a temperature coefficient of resistivity of 0.0019 K^{-1}, an adequate linear behavior, and a thermal product of 0.2 $J/cm^2/K/s^{½}$. Furthermore, the construction techniques produced gauges that were reliable, reproducible, and rugged. The results from shock tube tests showed that the RTDs had a time response on the order of microseconds and were suitable for making heat transfer measurements in highly transient conditions. Suggestions for further developments are included.

1.0 INTRODUCTION

Heat transfer is the dominant problem in the design of hypersonic vehicles. It also plays an important role in many other applications where experimental data is needed to support the design effort. Much of the data that is needed to support the design effort and to validate and calibrate numerical codes is generated from impulse facilities. When the flows of interest are generated in shock tubes, hypersonic shock tunnels or other short-duration facilities, the total flow time may be only a few milliseconds or less. In such cases the technique used for heat flux or temperature measurement must be suited for transient conditions and must have a response time fast enough to trace variations caused by rapidly changing flow conditions.

Thin film platinum resistance temperature detectors (RTDs) are suitable for measuring surface temperatures in flows of this nature. From the time history of the surface temperature, the heat flux may be obtained. These RTD gauges consist of thin metallic films applied to the surface of substrates of low thermal conductivity. The extremely small thickness of the gauges allows temperature measurements to be made with a time response of only a few microseconds. Furthermore, data from a properly mounted gauge can be reduced to obtain heating rates.

2.0 THIN FILM GAUGE PRINCIPLES

Principles of Thin Film Gauge Operation

The RTD operates on the simple principle that the resistance of metals increases with a rise in temperature. The method for determining heat transfer rates consists of measuring the temperature rise during the test time and calculating the heat flux from the data. When using RTDs, the surface temperature is determined from the change in resistance of the gauge film. For practical purposes, the resistance of platinum RTDs varies linearly with temperature as [1]

$$R(T) = R_0[1 + \alpha_R (T - T_0)] \qquad (2.1)$$

where R is the film resistance at surface temperature T, R_0 the film resistance at temperature T_0, and α_R is the film temperature coefficient of resistance which must be experimentally determined for each RTD.

Since there is a very small change in resistance for a given change in temperature, a Wheatstone bridge is used to increase the output sensitivity by using a nulling principle. During testing the bridge is supplied with a constant current. Thus a change in resistance of the RTD is converted to a change in voltage. In addition, the bridge ensures stability of the output by compensating for lead resistance[2]. Therefore, by using Ohm's law, when the film is

---

† Graduate Student, Member AIAA
‡ Associate Professor of Aerospace Engineering, Associate Fellow AIAA

supplied with a constant current the change in temperature is given by the equation

$$(T - T_0) = \frac{\Delta V}{\alpha_R V_0} \qquad (2.2)$$

where *DV* is the change in the film output voltage and V_0 is the initial voltage applied to the RTD. From equation (2.2) it is apparent that the gauge sensitivity is directly proportional to the voltage applied to the RTD. Therefore, the sensitivity of the gauge can be increased by operation at as high a film voltage as possible. However, the maximum excitation voltage that can be applied to the gauge is limited by internal heat generation. In order to minimize the errors introduced by this heat generation, a self-heating calibration test must be performed to determine this threshold.

Analysis

The basic time dependent problem of thin film gauges is conduction into a thin metallic film mounted on a semi-infinite extent of another material. Figure 2.1 shows the situation which must be analyzed. Theoretically, the film is infinitely thin so that it does not affect the temperature history of the substrate surface.

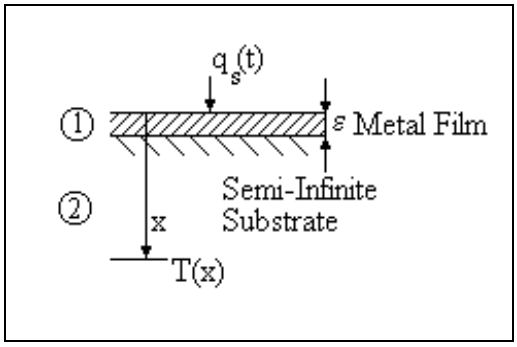

Figure 2.1. Heat Conduction In Thin Film RTD.

The equations that are used to calibrate RTDs and to calculate the heat flux from the temperature history are based on three main assumptions. It is assumed that the heat transfer is one-dimensional, that the substrate is semi-infinite, and that the measuring surface film has a negligible effect on the heat conduction. The first two assumptions are closely related in that the thickness of the substrate determines if one-dimensional theory may be applied. The third assumption is actually an approximation which introduces an error in the deduced heat flux. The amount of this error is a function of the thickness of the film. Each of these assumptions is discussed below.

One-dimensional Theory

If accurate heat flux measurements are going to be made, the RTD must follow the one-dimensional theory as best as possible. In order to achieve this, the substrates on which the thin film gauges are mounted must be thick enough so that the heat transfer into the substrate is similar to that into a semi-infinite solid. Furthermore, the films must be placed away from substrate discontinuities at distances equivalent to or greater than those required for a semi-infinite substrate behavior. The minimum thickness required can be obtained by considering the substrate base temperature to surface temperature ratio for the situation shown in figure 2.1. For constant heat flux into the surface, this ratio is [3]

$$\frac{T(x,t)}{T(0,t)} = e^{-\frac{x^2}{4\alpha t}} - \left(\frac{\pi}{\alpha t}\right)^{1/2} \frac{x}{2}\, \mathrm{erfc}\left(\frac{x}{2(\alpha t)^{1/2}}\right) \qquad (2.3)$$

where a is the thermal diffusivity of the substrate and x is the penetration depth.

Ideally, the temperature at the substrate base should be the same as ambient for all testing times. Therefore, at the end of a test, the ratio in equation (2.3) should be negligible. Figure 2.2 is a graph of the temperature ratio plotted as a function of the substrate depth for several different testing times. The thermal diffusivity of MACOR, a ceramic material used in this investigation, was used in the equation for plotting the temperature ratio.

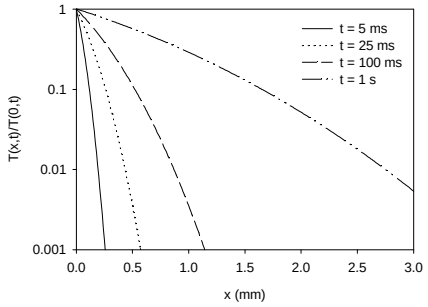

Figure 2.2. Determination of Minimum Substrate Thickness.

From the graph it can be seen that for a substrate base temperature to surface temperature ratio of less than 1% the substrate thickness must be about 3.0 mm

even for the relatively long testing time of about 1 second. However, for reasons of mechanical strength, insulating substrates are actually over 3 mm thick [4]. From the graph it is obvious that substrates which exceed this value are satisfactory for all durations less than about 1 second. Therefore, for short duration testing, the semi-infinite assumption is well satisfied.

Thin Film Thickness

Although the thin films deposited on the surface of insulating substrates are very thin, they have an effect on the surface temperature history which should be considered. If it is assumed that the films have no thermal capacitance, a large error could occur in the deduced heat flux if the testing time is significantly shorter than the response time of the RTD. For example, approximately 570 μs must elapse before the heat flux indicated by a painted platinum thin film having a thickness of about 1 μm approaches to within 5% of its correct value[4]. Therefore, care should be taken in the design and analysis of thin film heat flux experiments in short duration flow facilities. Since it is very difficult to measure the thickness of thin films, for the present investigation the thickness of the thin film gauges are assumed to be about 0.5 μm. This value is based on studies carried out by other investigators in which the average thickness of hand painted thin films was determined to be the stated value. In this case, about 100 μs is required before the accuracy in the deduced heat flux reaches 5% of its actual value[4].

Heat Flux Determination

In order to relate the measured temperature to the actual heat transfer rate, it is assumed that the thin film gauge has negligible heat capacity and that heat conduction in the substrate is one-dimensional into a semi-infinite solid of constant physical properties. Under these assumptions, the governing equations can be solved with the boundary conditions for the situation shown in figure 2.1 to give the surface temperature and heat flux to the surface as

$$T_s = \frac{1}{\sqrt{\pi}\sqrt{\rho ck}} \int_0^t \frac{\dot{q}_s(\tau)}{(t-\tau)} d\tau \qquad (2.4)$$

$$\dot{q}_s(t) = \frac{\sqrt{\rho ck}}{\sqrt{\pi}} \int_0^t \frac{\frac{dT}{d\tau}(\tau)}{(t-\tau)^{1/2}} d\tau \qquad (2.5)$$

During calibration of the RTD, a rectangular voltage pulse was applied to the RTD bridge. In effect, a constant heat flux is applied to the thin film. If the heat flux to the surface is constant, the surface heat flux can be determined by carrying out the integration in equation (2.4) and converting the surface temperature change to a voltage change by using equation (2.2) to give

$$\dot{q}_s = \left(\frac{\rho ck}{t}\right)^{1/2} \frac{\pi^{1/2}}{2} \frac{\Delta V}{\alpha_R V_0} \qquad (2.6)$$

where $(rck)^{1/2}$ is the thermal product of the film. From equation (2.6) it is easily seen that the voltage change caused by the imbalanced bridge circuit is directly proportional to the square-root of time.

If the heat flux is not constant, numerical techniques must be used in the calculation of the heat transfer rate. In order to reduce the error introduced by the uncertainty in the integral term, equation (2.5) can be integrated using the Cook-Felderman algorithm[5]

$$\begin{aligned} \dot{q}_n(t) = \frac{\sqrt{\rho ck}}{\sqrt{\pi}\alpha_R V_0} \Bigg[& \frac{V(t_n)}{t_n^{0.5}} \\ & + \sum_{i=1}^{n-1} \Bigg\{ \frac{V(t_n) - V(t_i)}{(t_n - t_i)^{0.5}} - \frac{V(t_n) - V(t_{i-1})}{(t_n - t_{i-1})^{0.5}} \\ & + 2\frac{V(t_i) - V(t_{i-1})}{(t_n - t_i)^{0.5} + (t_n - t_{i-1})^{0.5}} \Bigg\} \\ & + \frac{V(t_n) - V(t_{i-1})}{\Delta t^{0.5}} \Bigg] \end{aligned} \qquad (2.7)$$

where n is the number of equal divisions of time Dt and t ranges from 0 to nDt. Since equation (2.7) involves no integration approximations, the accuracy of the result obtained in using this expression is limited only by the degree to which the true voltage response is approximated by the piecewise linear expression. Furthermore, this algorithm avoids discontinuities at the endpoints of the temperature history due to start up and shut down transients during a test.

From equations (2.6) and (2.7) it is apparent that in order to perform heat flux calculations, it is necessary to first determine two thermal properties of the RTD: the thermal product and temperature coefficient of resistance. These thermal properties are determined

from static and dynamic calibration tests on the RTDs.

3.0 THIN FILM GAUGE CONSTRUCTION

The type of ceramic used as substrate material is MACOR, a machinable glass ceramic available from Corning Glass Works[6]. MACOR is an ideal substrate material because it has a low thermal conductivity. Good insulation properties are required to ensure the validity of the semi-infinite slab assumption. MACOR may also be heated to 1000°C without significant geometric deformation. Temperatures near this value are required during gauge preparation. Table 3.1 shows some of the thermal properties of MACOR compared with two other commonly used insulating substrate materials [4,6].

Table 3.1 Thermal Properties of Electric Insulators

Insulator	ρ (g/cm^3)	c (J/g/K)	k (J/cm/s/K)	$(\rho ck)^{1/2}$ (J/cm^2/K/s$^{1/2}$)
MACOR	2.52	0.790	0.0146	0.171
PYREX	2.22	0.775	0.0136	0.153
Quartz	2.21	0.755	0.0140	0.153

It should also be noted that this material may be machined easily so that gauges may be placed on complex geometrical shapes. Although MACOR is available in many different shapes, a small cylindrical substrate is suitable and convenient for constructing rapid response RTDs to be used in transient facilities. In the present experiment, solid rods about 10 mm long with a diameter of 1.6 mm were used.

The procedure used for constructing platinum RTDs on ceramic substrates includes substrate surface preparation, gauge material application and electrical lead connection. Each phase must be strictly followed if successful temperature measurements are to be obtained.

Substrate Surface Preparation

In order to apply the gauge material, the substrate must be smooth and highly polished. The resulting film should be between 0.1 and 1.0 micron thick and sharp irregularities should be removed to ensure a smooth film. To obtain a smooth, polished surface, #600 grain wet or dry silicon carbide sandpaper was first used. The smoothing was then continued using #1000 and #2000 grain sandpapers mounted on a rapidly rotating flat disk. This was performed for several minutes until the ceramic surface appeared visibly polished. Care was taken to ensure that the cylinder surface remained flat and level during polishing. The edges of the cylinder were then slightly chamfered using #2000 grain sandpaper with the RTD mounted in a rapidly rotating drill. Rounding of the edges is required to avoid wrapping the lead connections around sharp corners, which would result in poor electrical contact. In order to complete the smoothing process, a crocus cloth was used with the rotating flat disk. After the surface had been adequately polished, the ceramic piece was washed with water and placed under a heating lamp to dry.

The smoothing process is very important since any geometric discontinuities in the substrate material such as fine cracks or cavities may produce faulty sensors. Therefore, the surface of the substrate was examined using a UNITRON MR3-24 metallographic microscope before the gauge material was applied. Figures 3.1 and 3.2 are micrographs showing the surface roughness of two completed RTDs. These photos clearly show that polishing greatly improves the surface quality.

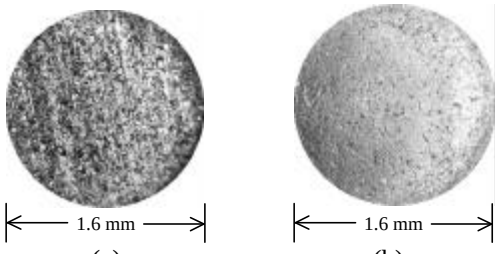

(a) (b)

Figure 3.1. Micrographs of Complete RTD Surface Taken at 17x a) #600 Grain Polishing b) Final Cloth Polishing.

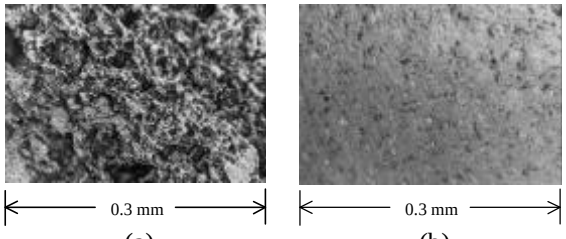

(a) (b)

Figure 3.2. Micrographs of a Section of the RTD Surface Taken at 66x a) #600 Grain Polishing b) Final Cloth Polishing.

Gauge Material Application

After the substrate surface had been adequately polished, the platinum film was applied. Platinum films are formed on insulating substrates by using commercially available preparations of metallo-organics such as "Liquid Bright Platinum 05-X" from Engelhard Industries. Metallo-organics are solutions of metal compounds in organic solvents. The liquid contains fine metallic particles in suspension and chemical agents that attack the surface of the substrate to provide a highly adherent film. Table 3.2 contains some of the thermal properties of platinum compared with two other commonly used gauge materials[4].

Table 3.1 Thermal Properties of Electric Conductors

Insulator	r (g/cm^3)	c (J/g/K)	k (J/cm/s/K)	$(rck)^{½}$ (J/cm^2/K/s^{½})
Platinum	21.5	0.13	0.70	1.40
Nickel	8.90	0.45	0.84	1.83
Copper	8.90	0.38	3.97	3.66

Before application to the substrate, the Liquid Bright Platinum solution was mixed with the thinning essence toluene. Several factors must be considered when preparing the solution, including purity, concentration, and film thickness. The materials should be mixed in a clean environment since any impurities introduced during the mixing may result in faulty gauges. Figure 3.3a shows the effects of mixture impurities on the completed film surface. The relative concentration of the platinum and thinner is also important because the final resistance of the gauge depends strongly on the amount of platinum deposited on the surface. Furthermore, poor adhesion may arise from too thick an application of liquid (figure 3.3b). Therefore, the liquid should be thin enough for brush marks to flow out and take on a luster. During the present investigation it was found that a mixture of three parts thinner and one part liquid bright platinum applied using a small brush with fine hairs produces the best films.

The preferred method for applying the platinum films to the substrate surface consisted of painting a strip of platinum about 0.8 mm wide on the surface of the substrate. In order to ensure uniform film thickness, a single stroke was used. Although regulating the amount of platinum applied to the surface is difficult, this method ensures the validity of the one-dimensional analysis assumption.

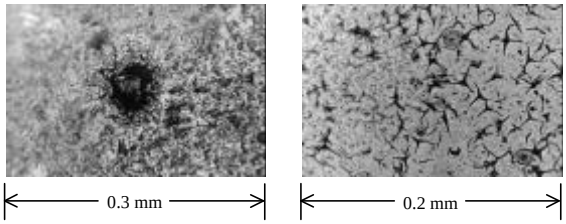

Figure 3.3. Micrographs Taken at 66x and 100× Showing a) Effects of Impurities on Film Surface b) Cracking Due to Film Thickness Surface.

Immediately after application of the platinum, the gauges were dried by a high power lamp. The total drying time under the lamp ranged between 10 and 20 minutes. Drying was performed in a clean environment to avoid the collection of dust or other impurities on the gauge surface.

In order for the liquid platinum to form on the surface of the substrate, the piece must be baked at very high temperatures to remove the carrier. The substrates were supported on a steel base which had been pre-baked and inserted into an electric furnace. The temperature was gradually increased to 750°C over about one hour and maintained at that temperature for a further thirty minutes. During firing, it is necessary that the rate of increase be gradual so that blistering or boiling of the film does not occur.

After baking, the RTDs were cooled slowly overnight in the furnace in order to avoid cracking. These cracks may cause the film's resistance to increase with time due to stress relief. For properly constructed gauges, the final film resistance should be 75–150 ohms.

Lead and Electrical Connections

The thin film leads to the platinum film were made using the metallo-organic solution "Liquid Bright Gold NW" from Engelhard Industries. Gold is a convenient material for thin film platinum gauges because the same baking temperatures and times may be used as for platinum. It should also be noted that gold forms thin film connections, in contrast to other materials such as silver, which forms thick film connections with possible surface discontinuities[7].

The gold leads were applied to the middle of the ceramic rod. It is not necessary to polish the outer surface of the rod, but it must be clean and dry. The liquid gold was painted on the outer surface of the

ceramic rod in thin strips on opposite sides of the piece. The gold leads were made using a single stroke of a small paint brush starting about halfway down the ceramic piece and ending at the edge of the platinum film. The gold ink was applied with the ceramic piece in a horizontal position to ensure adequate material for conduction. After application of the gold strips, the piece was dried and baked as described above.

When applying the gold leads, very careful attention must be given to the interface where the two metals meet. The overlap point between the metals must be kept to a minimum. If too much gold is applied to the film, the resistance of the film will be lowered by shortening its effective length. Since the diameter of the RTD surface is only 1.6 mm, a small amount of gold on the surface could significantly lower the resistance. However, care must be taken to ensure that an adequate amount of gold is applied at the interface between the two metals. During calibration, it is necessary to subject the RTD to a voltage pulse of about 6 V. If there is not enough gold at the contact point, or if the edge is not adequately rounded, burnout will occur and the gauge will fail.

The final step in gauge construction is making electrical connections to the gold leads. Uninsulated constantan thermocouple wire (Omega SPCI–003) with an outer diameter of 0.3 mm was used for making the connections. The wires were attached to the gold leads using a silver loaded epoxy adhesive Epo-Tek H20E available from Epoxy Technologies. Following application, the epoxy was cured in an oven at a temperature of 150°C for 30 minutes. Electrical tape was then used to insulate the gold leads and to increase the structural stability of the wire leads. Figure 3.5 is a drawing of a completed thin film RTD.

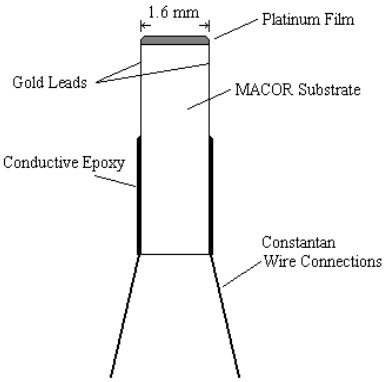

Figure 3.5. Thin Film RTD.

4.0 THIN FILM GAUGE CALIBRATION

Thin film heat transfer measurements require an accurate knowledge of the thermal properties of the gauge material. For example, the temperature resistance coefficient of a thin film gage depends on a variety of factors including the film material, the size of the deposit, and its shape. The useful linear range also depends on a number of factors including the uniformity of the metallic layer, purity and bonding to the substrate. Furthermore, the value of the thermal product depends on the history of the gauge construction and in particular the firing details of the ceramic production process[7]. Therefore, each RTD was calibrated independently since reproduction of films which are exactly the same is not feasible.

Self-Heating Threshold

The excitation current to an RTD must be below a threshold value to prevent appreciable ohmic heating. This threshold is determined by a self-heating test. The Wheatstone bridge was balanced and the RTD was placed in still air. The supply from a Hewlett-Packard Model E3630A triple power supply was slowly increased while the output voltage was measured. If there were no ohmic heating, the RTD resistance would not change and the output voltage would be zero since the bridge was initially balanced. Therefore, when self-heating occurs, a voltage will be measured.

Static Calibration

Once the threshold of self-heating was determined, static calibration was performed to determine the temperature coefficient of resistance. This test was also performed to determine the sensitivity and linearity of the RTD. The RTD was immersed in a 400 mL beaker filled with 99.99% pure glycerin and placed on a domestic heating element. Glycerin provides a stable medium and does not contain dissolved oxygen or other corrosive gases which may complicate interpretation of the results. Furthermore, glycerin has a very high boiling point compared to water which allows tests to be performed over a wider range of temperatures. A Radio Shack Model 22-174A multimeter was used to calibrate the RTD against an OMEGA Model CAIN-316(E)-12 Type K thermocouple probe from ambient to 120°C. This range more than adequately covers the temperature rises encountered in shock tube experiments.

Through experience it was found that maintaining a constant bath temperature during readings is vital. This is easiest when the bath is being cooled between readings. If constant bath temperatures are maintained during readings, the accuracy of the calibration is governed by the accuracies of the multimeter and thermocouple.

A least-squares, linear regression was performed on the data to determine the temperature coefficient of resistivity using the relationship

$$\alpha_R = \frac{1}{R_0}\frac{\Delta R}{\Delta T} \tag{4.1}$$

where R_o is the resistance of the film in ambient conditions. Accurate determination of both steady-state and transient heat transfer rates is dependent on the value of the temperature coefficient. Although, equation (4.1) is the expression which is used to determine this value, it should be noted that R_o is the resistance of the film at ambient conditions. If the conditions in which the static calibrations are performed are different than those which exist during actual testing, the value of R_o should be obtained from the test conditions. If this adjustment is not made, an error of about 1% in the measured heat flux could result for a temperature difference of about 5 to 10 °C[7].

Dynamic Calibration

Due to the interpenetration of platinum and ceramic that occurs at the interface between the thin film and the substrate, the physical quantities *k*, *r*, and *c* are not the properties of the bulk material. Therefore it is impossible to determine the thermal product by a standard steady-state method with any acceptable degree of accuracy and a transient technique must be used. In order to accurately determine the value of the thermal product, it was necessary to perform a double electrical discharge calibration. The double calibration technique was used to minimize errors which are introduced by non-uniform film heating and other affects.

The RTD was incorporated into a Wheatstone bridge and supplied with a rectangular voltage pulse of 6 V for 5 milliseconds using a Hewlett-Packard Model E3630A triple power supply. The pulse caused ohmic heating within the film and produced a change in resistance which was recorded as a change in output voltage. The resulting output voltage caused by the imbalanced bridge circuit was monitored with a Hewlett-Packard 54540A digital recording oscilloscope. This voltage response is equivalent to the temperature-time history of the gauge. Furthermore, from equation (2.6) it is known that for a constant heat transfer rate to the surface, the temperature change is a square-root function of time.

The test was first conducted in still air, where the heat loss to the surroundings was negligible in comparison with heat transferred by conduction to the substrate. A plot was then generated of the response voltage as a function of the square-root of time and a least-squares, linear regression was performed to determine the slope of the data. The test was then repeated with the RTD immersed in glycerin, where a fraction of the heat generated diffused into the liquid. A similar plot was obtained from which the slope of the transformed response was determined. The thermal product was then calculated from the relationship[7]

$$(\rho ck)^{1/2} = \frac{(\rho ck)^{1/2}_{gly}}{\dfrac{\left(\Delta V / t^{0.5}\right)_{air}}{\left(\Delta V / t^{0.5}\right)_{gly}} - 1} \tag{4.2}$$

where the thermal product of glycerin was obtained from Ref. 4.

Care must be taken in the use of the electrical pulse calibration procedure to reduce potential errors. The bridge circuit must be carefully balanced before each test. An initial imbalance of the bridge circuit will result in a step in the response output at the start of the test. This appears as an infinite heat transfer rate. The bridge circuit must also be as inductance free as possible so that oscillatory responses are either avoided or rapidly damped. Furthermore, the duration of the test must be short enough to ensure the validity of the one-dimensional assumption.

5.0 EXPERIMENTAL PROGRAM

Test Facility

The experiments were performed in the pilot shock tube at The University of Texas at Arlington's Aerodynamics Research Center. The tests were performed in order to determine the response time of the RTDs and to confirm that the devices may be used for making heat flux calculations in short

duration facilities. A brief description of the shock tube and set up is given below.

Shock Tube

The UT Arlington pilot shock tube is made of stainless steel, with a 100 mm ID driver tube and 50 mm ID driven tube connected by a convergent diaphragm section (figure 5.1). The driver section is separated from the driven section by a diaphragm. In the present experiment, Mylar diaphragms, 0.5 mm thick, without scoring were used. These diaphragms burst if subjected to a pressure difference of 2 ± 0.07 MPa. The driven section of the tube was subject to ambient conditions for all test runs. Air to the driver tube was regulated to 2.0 ± 0.07 MPa. The driver section pressure, p_4, was measured by a Wika Glycerin pressure gauge with ±70 kPa accuracy. Accurate measurements of p_4 are actually not necessary because the input pressure pulse can be obtained from accurate measurements of shock speed (M_s), driven-tube pressure (p_1) and temperature (T_1). A run was initiated when the Mylar diaphragm separating the driven- and driver-tube was burst.

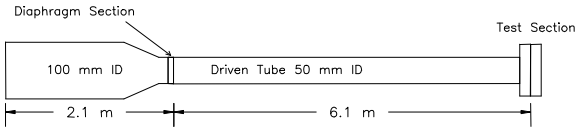

Figure 5.1. Pilot Shock Tube.

Test Section

The test section, located at the downstream end of the driven tube, was instrumented with two wall mounted pressure transducers and an RTD mounted in a probe (figures 5.2 and 5.3). The test probe consisted of the three parts shown in figure 5.2. Before mounting the RTD into the probe it was necessary to electrically insulate the gold and wire leads. Electrical tape was used to carefully cover any exposed leads. The RTD was then inserted into the teflon casing so that the film surface protruded approximately 1/8" out of the casing. The teflon casing was made slightly larger than the hole it was inserted into in the probe tip. Therefore, when the casing was pressed into the probe tip it constricted tightly around the RTD holding it firmly in place. This was necessitated by the high pressures encountered in the shock tube which could force the RTD out of the probe. Care was taken during the mounting of the RTD into the probe tip to ensure that the film was flush with the contour of the probe. The copper probe tip was then mounted onto the probe body which was attached to the shock tube end plate.

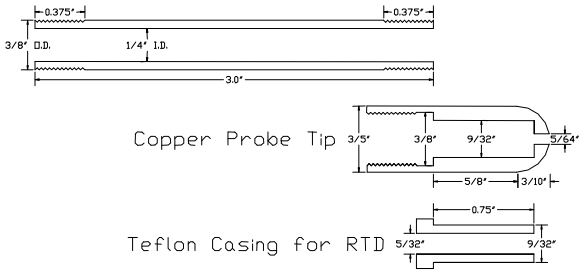

Figure 5.2. Probe Design.

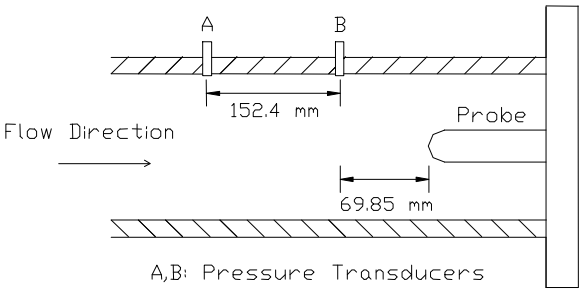

Figure 5.3. Pressure Transducer and RTD Mounting.

The pressure transducers were used to measure the shock speed and to determine the precise time the shock passed over the RTD. Experiments[8] indicate that theoretically computed shock strengths are higher than those actually attained. Initially, the diaphragm burst delays the formation of a one-dimensional shock wave. Then as the wave moves down the tube it decelerates due to boundary layer growth. Therefore, the shock speed must be measured to evaluate the actual local shock strength. Shock speeds can be determined by finding the lapsed time of the wave as it passes two points.

In this experimental program, two 13.8 MPa PCB piezoelectric pressure transducers were flush-mounted in the tube wall precisely 152.4 mm apart. The shock Mach number was then computed as

$$M_s = \frac{\left(L/\Delta t\right)}{a_1} \tag{5.1}$$

where a_1 is the ambient speed of sound of the driven tube, Dt is the lapsed time of the wave, and L is the distance between the two transducers. Once the shock speed and the driven-tube pressure and

temperature were known, the input pressure pulse was obtained as[9]

$$p_2 = p_1\left[1+\frac{2g}{g+1}(M_s^2-1)\right] \qquad (5.2)$$

where γ is the specific-heat ratio. Furthermore, equation (5.3) was used to calculated the resulting temperature rise due to shock passage[9]

$$T_2 = T_1\left[\frac{\left(1+\frac{\gamma-1}{2}M_1^2\right)\left(\frac{2\gamma}{\gamma-1}M_1^2-1\right)}{M_1^2\left(\frac{2\gamma}{\gamma-1}+\frac{\gamma-1}{2}\right)}\right] \qquad (5.3)$$

Shock-Tube Experiment

A Hewlett-Packard Model 54540A, four-channel, digital recording oscilloscope with a maximum sampling rate up to 500 MSa/sec per channel was used to gather pressure and temperature data. In the present experiment three channels were used to capture data at a sampling rate of 1 Megasample/second per channel. Channels 1 and 2 were used to gather data from the PCB pressure transducers, while channel 4 monitored the RTD response. The RTD was again used in conjunction with the Wheatstone bridge and supplied with an excitation of 2 V from a Hewlett-Packard E3630A triple power supply. The pressure transducers were powered by a Model 482A04 I.C.P. 24 V power supply. All input channels were triggered simultaneously by an external trigger source. The external trigger consisted of a soft, thin wire placed flush with the Mylar diaphragm on the upstream side. The wire was supplied with 5 V from a Hewlett-Packard 6235A triple power supply. Triggering occurred when the diaphragm ruptured causing the wire to break and resulting in a sharp decline in the voltage measured by the external trigger channel of the oscilloscope. After observing the speed of a typical shock wave, a delay was set on the oscilloscope in order to focus in on the test section of the run.

6.0 RESULTS AND DISCUSSION

The results of the construction techniques, the calibration results, and the verification tests are discussed in this chapter. Ten samples were chosen from the RTDs produced and are considered representative of all of the hand-made gauges. Five RTDs were chosen from those produced using the method of coating the entire surface of the RTD with platinum, and five were chosen produced by painting a single strip of platinum on the substrate surface. Only samples that had final resistance values of between 75-150 ohms were calibrated and tested.

Construction Techniques

During the initial trial-and-error phase of the construction process, only about 10% of the RTDs produced had the desired resistance. Due to the rapid evaporation of the thinning essence and the inability to closely regulate the platinum contained in the brush, the final resistance values were consistently too low. Out of these 10%, nearly all were destroyed when subject to excitation voltages as low as 2 V. This was caused by an inadequate amount of lead material at the platinum contact point which resulted in burnout. After gaining a considerable amount of experience, the success rate was increased to about 90% for the RTDs produced by painting the single strip of platinum. Although the amount of platinum applied could not be easily regulated, this method proved to give more consistent and reliable results.

The construction techniques also produced RTDs that were reliable and rugged. Final shock tube testing showed that reliable heat transfer rates could be obtained using the thin film gauges. Furthermore, a test was performed to determine the effects of repeatedly subjecting the sensors to the harsh testing environment. After eight test runs the thin film showed no signs of deterioration and the film resistance remained constant.

Self-Heating

Figure 6.1 shows the results of the self-heating test. The test shows that the output is practically zero up to an excitation of about 1 V, above which the effects of ohmic heating on the RTD become apparent. However, up to an excitation of about 2 V, the effects are minimal and can be accounted for in the final calculations. Although the false signal due to the ohmic heating is not negligible for an excitation of 2 V, it should be recognized as an offset that can be set equivalent to the ambient conditions. Since the sensitivity of the RTD is a function of the voltage supplied to the bridge circuit, it is recommended that 2 V be used as the excitation threshold. Input values greater than this cause the internal heat generation to

increase rapidly and burnout usually occurs before an excitation of 4 V is reached.

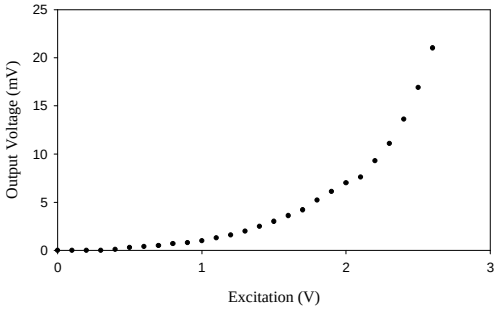

Figure 6.1. Threshold of Self-Heating in Air.

Static Calibration

Figures 6.2 and 6.3 show the static calibration results. The sensitivities of each of the RTDs were determined by a first-order least-squares curve fit. In each case the value of the correlation coefficient was calculated and found to be better than 0.99. The nearly perfect correlation in every case was achieved by very carefully measuring the temperature of the glycerin and the resistance of the RTD as the bath was cooling. This was a time consuming process that was useful in confirming the expected linear behavior over the temperature range tested. The linear behavior of the RTDs confirms that they can be used to make precise measurements without complicated data reduction proceduces.

For experimental purposes it is desired that the sensitivity of the RTD be as high as possible so that accurate measurements can be made. When a correlation of the sensitivity data was performed it was found that as the resistance of the RTD increased, the sensitivity increased. Figure 6.4 is a plot of the sensitivity as a function of film resistance. From the graph it is apparent that there is an increasing linear trend with the data. An interesting characteristic of thin platinum films is that as more material is applied the resistance decreases. Similarly, as the amount of material applied to the surface of the RTD is decreased, the resistance increases. Therefore, this increasing linear trend can be accounted for by the decrease in gauge material.

During testing, the sensitivity of the RTD was increased by using a Wheatstone bridge and rapid changes in temperature were measured with a high-speed digital oscilloscope. It was therefore necessary to know how the sensitivity varied as a function of the excitation supplied to the bridge. Furthermore, the output voltage as a function of increasing temperature had to be known. From figure 6.5 it can be seen that the sensitivity is a linear function of the excitation and that the sensitivity is significantly increased by the use of a Wheatstone bridge.

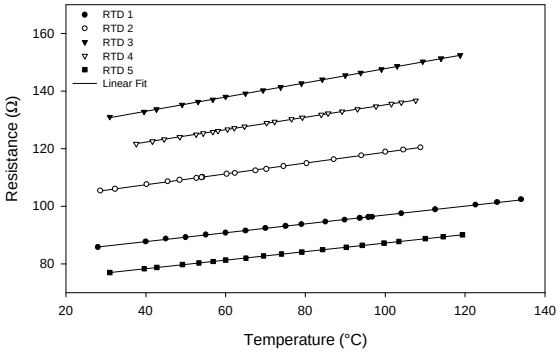

Figure 6.2. Static Calibration for RTDs 1–5.

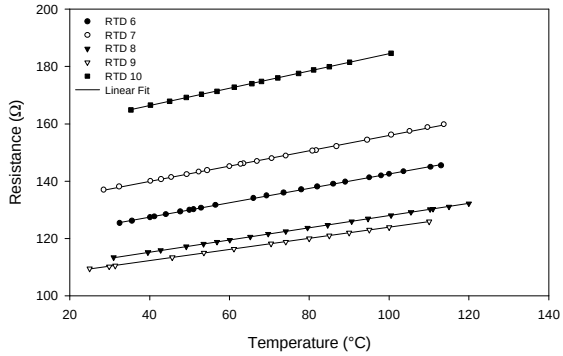

Figure 6.3. Static Calibration for RTDs 6–10.

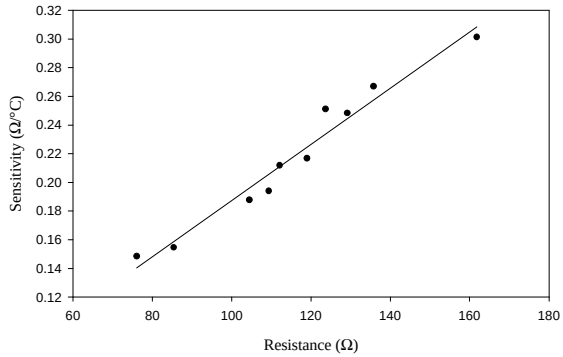

Figure 6.4. Correlation of RTD Sensitivities.

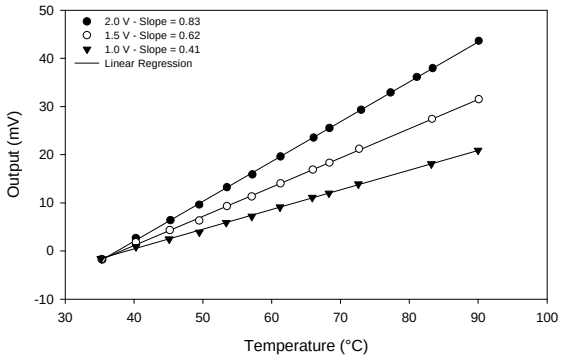

Figure 6.5. RTD Sensitivity.

Table 6.1 contains the tabulated data shown in figures 6.1 through 6.5 along with the temperature coefficient of resistance for each RTD and the error analysis results. For each case, the coefficient of resistance was calculated using equation (4.1) with the resistance of the RTD taken at 25°C. The error of approximately one percent for each RTD shows that the calculated values are very accurate. If precise heat flux measurements are needed, the coefficient should be calculated from the resistance of the RTD at the initial testing temperature.

Table 6.1. Static Calibration Results

RTD	Ω at 25°C	a_R (K^{-1})	% Error	Sensitivity (Ω/°C)	r
1	85.4	0.00181	1.24	0.155	0.9997
2	104.6	0.00182	1.35	0.188	0.9993
3	129.3	0.00191	0.95	0.247	0.9998
4	119.0	0.00182	1.35	0.217	0.9999
5	76.1	0.00195	1.55	0.148	0.9999
6	123.7	0.00203	1.02	0.251	0.9999
7	135.9	0.00198	0.91	0.267	0.9997
8	112.1	0.00189	1.09	0.212	0.9999
9	109.4	0.00178	1.24	0.194	0.9998
10	161.8	0.00186	1.07	0.301	0.9999

Dynamic Calibration

Electrical discharge calibrations were performed to determine the thermal product of each RTD. The magnitude of the rectangular voltage pulse was varied from 3 V to 20 V to determine an acceptable excitation value. For excitation values less than about 4 V there was very little bridge response due to RTD ohmic heating. With 5 – 10 V excitation, the RTD response was adequate for performing dynamic calibrations and the thermal product values were consistent throughout this range. Excitation values greater than 10 V also produced adequate results, but there was a high rate of failure due to RTD burnout which increased rapidly with increasing voltage. Furthermore, as the voltage was increased, small deviations from a perfectly balanced bridge were greatly magnified. Although this did not affect the final value of the thermal product, in some cases the oscilloscope scale had to be reset in order to capture the increased response values. For the ten RTDs in this experimental program, only the data for the 6 V excitation are presented.

Figure 6.6 shows the results of the dynamic calibration. As discussed in section 4.3, a rectangular voltage pulse heats the RTD such that the bridge circuit response should ideally follow a square-root function of time. The figure includes a least-squares square-root of time behavior of the data, with a correlation coefficient of 0.99.

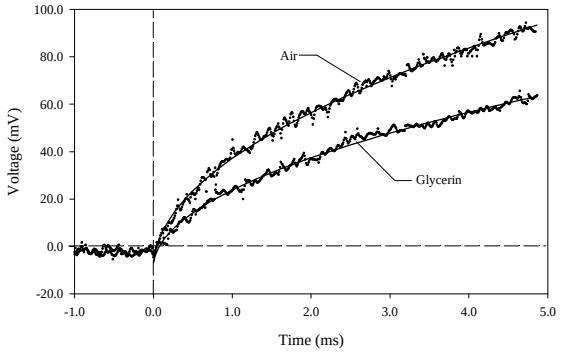

Figure 6.6. Dynamic Calibration Results.

The square-root of time behavior is further shown in figure 6.7, which confirms the theory presented in section 4.3. The figure also contains confidence intervals that are used to estimate the error in the data. From the graph it is apparent that there is very little error introduced by the linear approximation to the data. Table 6.2 contains the tabulated dynamic calibration data for each RTD including the thermal product and the calculated correlation coefficients.

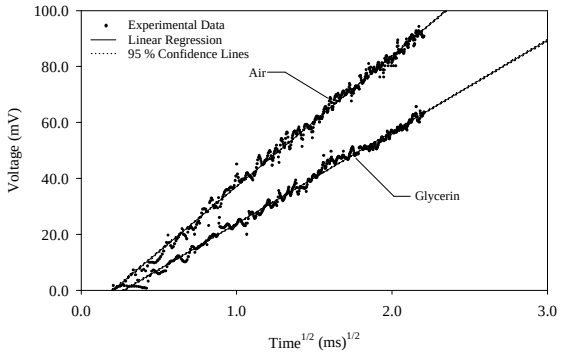

Figure 6.7. RTD Response After Square-root Transformation.

Table 6.2. Dynamic Calibration Results.

RTD	Ω at 25°C	$(rck)^{½}$ (J/cm^2/K/s^{½})	Air Correlation Coefficient	Glycerin Coefficient
1	85.4	0.205	0.9961	0.9954
2	104.6	0.191	0.9818	0.9670
3	129.3	0.193	0.9829	0.9672
4	119.0	0.200	0.9963	0.9963
5	76.1	0.193	0.9913	0.9909
6	123.7	0.190	0.9938	0.9938
7	135.9	0.213	0.9948	0.9911
8	112.1	0.207	0.9947	0.9901
9	109.4	0.216	0.9954	0.9963
10	161.8	0.215	0.9960	0.9917

RTD Testing

Two RTDs were employed for determining heat transfer rates in a known flow, namely, the stagnation point heat transfer to a hemisperical cap. This enabled their performance to be evaluated against a theoretical benchmark. To accomplish this, an RTD was carefully mounted in the tip of the probe shown in figure 5.2 and placed in the shock tube along with two PCB pressure transducers as shown in figure 5.3. Figure 6.8 is a plot of the pressure transducer outputs during a test run. The first time lapse shown on the graph indicates the passage of the incident shock wave, while the second indicates the passage of the reflected shock from the downstream end of the tube. The time elapsed for the oncoming shock to travel between the two transducers was 246 ± 2 μs. Therefore, the experimental shock Mach number was determined to be 1.79 ± 1 percent using equation (5.1). The shock speed was 619.5 m/s ± 1 percent. Using this velocity and knowing the distance between the RTD and transducer "B" (figure 5.3), the time of arrival of the shock was found to be 113 ± 2 μs after passing transducer "B". Therefore, the time the shock contacted the RTD surface was calculated as 8.975 ± 0.003 ms.

In order to determine the testing time, it was necessary to consider the influence of both the reflected shock and the contact surface. The passage of either of these surfaces would cause an appreciable change in the temperature of the air.

As shown in figure 6.8, the time elapsed for the reflected shock to travel between the two transducers was 503 ± 2 μs. This gave a reflected shock Mach number of 0.87 ± 1 percent which corresponds to a speed of 304.6 m/s ± 1 percent. Using this velocity and the geometry of the configuration, it was determined that the reflected shock passed over the RTD surface at 9.464 ± 0.003 ms.

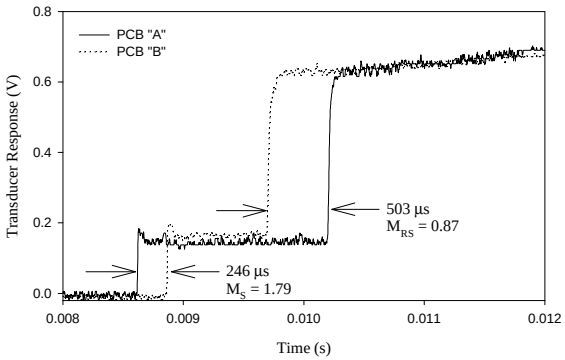

Figure 6.8. Shock Speed and Test Time Determination.

The time that the contact surface passed over the RTD surface is not precisely known. However, an estimation was calculated by first determining the theoretical speed of the contact surface using the equation[10]

$$u_p = \frac{a_1}{g_1}\left(\frac{p_2}{p_1} - 1\right)\left(\frac{\frac{2g_1}{g_1+1}}{\frac{p_2}{p_1} + \frac{g_1-1}{g_1+1}}\right)^{0.5} \qquad (6.1)$$

From equation (6.1) the speed of the contact surface was estimated to be 355.2 m/s. The actual speed of

the contact surface was probably less than this due to boundary layer growth. Therefore, equation (6.1) is actually the limiting case and can be used to determine the test time. Using the velocity of the contact surface and knowing the distance between the RTD and diaphragm section, the arrival of the contact surface was estimated to be 16.9 ms. The shock trajectory and contact surface interaction are shown graphically in figure 6.9.

Since the reflected shock passed over the RTD much sooner than the estimated time of the contact surface, the test time was determined to be approximately 489 ± 4 μs by simply taking the difference between the initial and reflected shock passage times. This testing time was deemed of adequate length for this experiment.

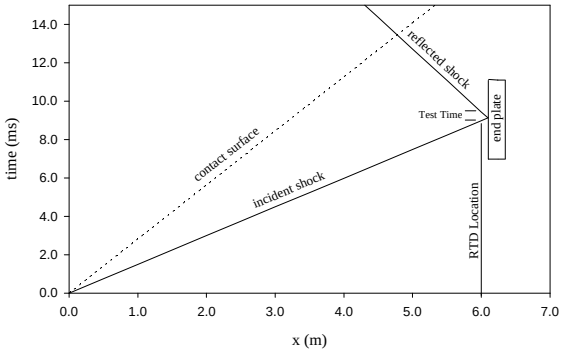

Figure 6.9. Shock and Contact Surface Interaction.

Figure 6.10 is a plot of the response of RTD 9 showing about 1 ms of data before passage of the shock wave and the following 3 ms. For this run, data was taken at a rate of 1 MSa/s. In order to convert the RTD response from a voltage reading to a meaningful temperature measurement, 1 ms of data prior to shock passage was averaged and set equivalent to the ambient temperature of 25°C. The sensitivity of the RTD when subjected to an excitation of 2 V was then used to convert the response voltage into a temperature measurement.

Heat Flux Determination

Three techniques were used to compute the stagnation-point heat transfer rate and compared with one another for accuracy. Two of the methods used the experimental data obtained with the RTDs and the third method was based on theory. Each method is described below and the results that were obtained are presented.

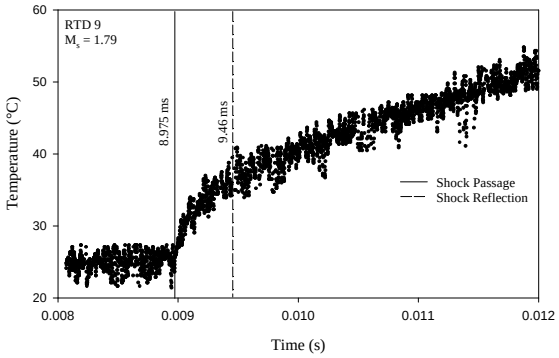

Figure 6.10. RTD Response.

Constant Heat Flux Case

The first method used was based on the assumption that the heat transfer rate was constant over the test time. Using this assumption, equation (2.6) was rearranged to give the change in voltage as

$$\Delta V = \left(\frac{2\alpha_R V_0}{(\rho c k)^{1/2}} \right) \dot{q}_s t^{1/2} \qquad (6.2)$$

As discussed in section 2.3, if the heat flux is constant the voltage change caused by the imbalanced bridge circuit should ideally be directly proportional to the square-root of time. It was therefore necessary to shift the time scale of the experimental data so that the shock wave passed over the RTD at time zero. A plot of the RTD response as a function of the shifted square-root of time is shown in figure 6.11.

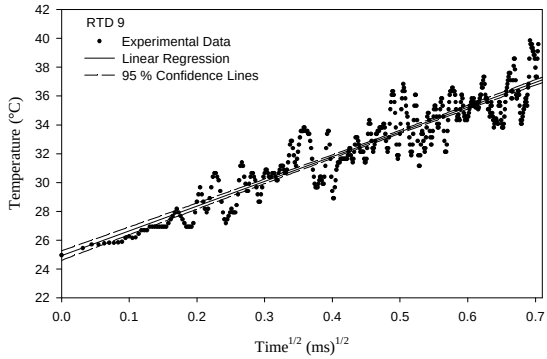

Figure 6.11. Transformed Temperature Response of RTD 9.

After shifting the time scale and plotting the response as a function of the square-root of time, a linear

regression was performed on the data to obtain an equation of the form

$$\Delta V = \lambda t^{1/2} + c \tag{6.3}$$

where l is the slope of the regression line and c is a constant due to an initially imbalanced bridge. By noting that c is only an offset from the origin which can be set equal to zero without affecting the slope, equations (6.2) and (6.3) were equated to yield an equation for the constant heat transfer rate as

$$\dot{q}_s = \left(\frac{(\rho c k \pi)^{1/2}}{2\alpha_R V_0} \right) \lambda . \tag{6.4}$$

By using the values of the thermal product ($\sqrt{\rho c k}$ = 0.216 J/cm^2/K/s$^{1/2}$) and the temperature resistance coefficient (α_R = 0.00178 K^{-1}) obtained during the calibration of RTD 9, the stagnation-point heat transfer rate was found to be 23.2 W/cm^2 ± 11 percent.

Fay-Riddell Correlation

The second method was used as a theoretical check of the experimental results. This method is based on the work of Fay and Riddell. They determined that the theoretical curve-fit for the stagnation-point heat transfer rate for a laminar boundary layer of a spherical cap is given by[11]

$$\dot{q}_{t,ref} = \frac{0.763}{(Pr_{w,t})^{0.6}} (\rho_{t2}\mu_{t2})^{0.4} (\rho_{w,t}\mu_{w,t})^{0.1} (H_{t2} - h_{w,t}) * \left[1 + (Le^{0.52} - 1) \frac{h_d}{H_{t2}} \right] \left[\left(\frac{du_e}{dx} \right)_{t2} \right]^{0.5} \tag{10}$$

where r is the density, m is the viscosity, H is the stagnation enthalpy, h is the static enthalpy, Le is the Lewis number, Pr is the Prandtl number, and du_e/dx is the stagnation-point velocity gradient. However, the bracketed term containing the Lewis number is only needed when the temperatures and temperature gradients are sufficiently high so that appreciable dissociation and concentration gradients across the boundary layer are present. Furthermore, the stagnation-point velocity gradient of a hemisphere is given by[11]

$$\left(\frac{du_e}{dx} \right)_{t2} = \frac{1}{R_N} \sqrt{\frac{2(P_{t2} - P_\infty)}{\rho_{t2}}} \tag{6.5}$$

where P is the pressure and R_N is the nose radius. Therefore, the equation for the heat-flux becomes

$$\dot{q}_{t,ref} = \frac{0.763}{(Pr_{w,t})^{0.6}} (\rho_{t2}\mu_{t2})^{0.4} (\rho_{w,t}\mu_{w,t})^{0.1} * (H_{t2} - h_{w,t}) \left[\frac{1}{R_N} \sqrt{\frac{2(P_{t2} - P_\infty)}{\rho_{t2}}} \right]^{0.5} \tag{6.6}$$

where *t2* denotes the conditions at the stagnation point downstream of a shock wave, *w* the surface conditions, *t* the stagnation-point value, and ¥ the freestream conditions.

When using equation (6.6), the density and enthalpy were computed using the perfect gas relations, the Prandtl number was assumed to be 0.7, and the downstream pressure was calculated using equation (5.2). Furthermore, the viscosity was calculated using Sutherland's Law as[12]

$$\mu = \mu_\infty \left(\frac{T}{T_\infty} \right)^{0.5} \frac{1 + 0.505}{1 + 0.505 \frac{T}{T_\infty}} \tag{6.7}$$

where T was calculated using equation (5.3).

By going through the above analysis, the theoretical value for the stagnation-point heat transfer rate for a laminar boundary layer of a spherical cap was found to be 26.2 W/cm^2 ± 3 percent. This is only 13 percent greater than the experimentally calculated heat transfer rate which had an error of ± 11 percent. Therefore, the RTD was considered to give reliable heat transfer rate results.

Cook-Felderman Algorithm

The final method used to calculate the heat-transfer rate was the Cook-Felderman algorithm discussed in section (2.3). It was found that when using this method the raw RTD response data could not be used because of the noise present within the data. The sharp fluctuations in the RTD response caused large errors in the calculated heat transfer rate. Furthermore, the algorithm failed to converge on an approximate heat transfer rate value. However, the

algorithm proved useful for calculating the heat transfer rate from data that the random noise has been removed from.

Figure 6.12 shows the RTD response with a parabolic fit that was determined from the least-squares square-root of time regression line shown in figure 6.11. Using this parabolic fit data along with Cook-Felderman algorithm given in equation (2.7), the heat flux was determined numerically.

Figure 6.13 is a plot of the heat flux results that were calculated using all three methods. Although the testing time was only about 0.5 ms, the graph shows a time of 1 ms. The longer time was need to show that the Cook-Felderman algorithm actually converges to a value which is very close to the theoretically calculated value of 26 W/cm^2.

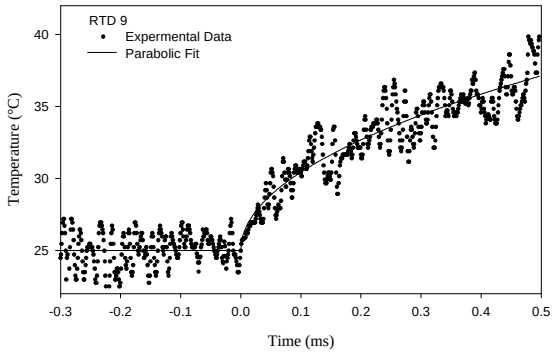

Figure 6.12. Temperature Response of RTD 9.

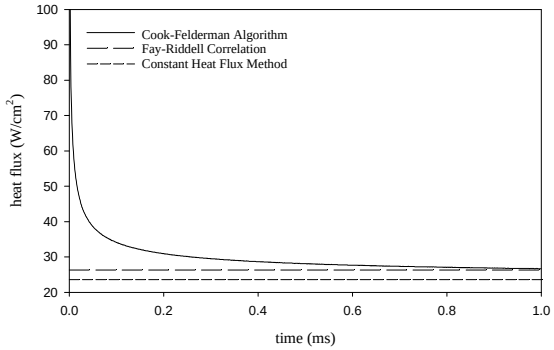

Figure 6.13. Heat Flux Correlation for RTD 9.

Repeatability

The repeatability of the experiments was checked by performing the same shock tube tests under similar conditions with a different RTD. The same methods as presented above were used to determine the heat flux. Figure 6.14 shows the response of the RTD as a function of the square-root of time with a least-squares linear regression line and 95 percent confidence intervals. The results of the analysis for the two RTDs are tabulated in table 6.3.

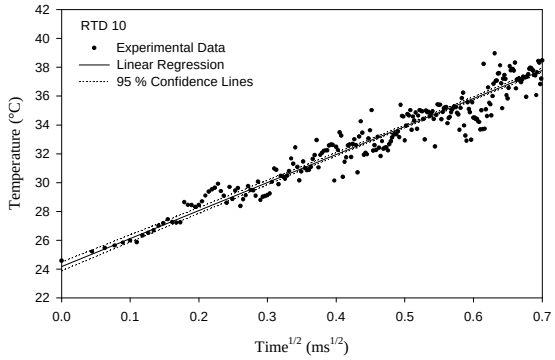

Figure 6.14. Transformed Temperature Response of RTD 10.

Table 6.3. Calculated Heat Flux Results

RTD	Constant Heat Flux Case (W/cm^2)	Fay-Riddell Method (W/cm^2)	Cook-Felderman @ t = 1 ms (W/cm^2)
9	23.22 ± 11 %	26.2 ± 3 %	28.1
10	25.08 ± 10 %	27.0 ± 3 %	29.8

CONCLUSIONS AND RECOMMENDATIONS

Conclusions

The objective of the investigation was to construct, calibrate, and test hand-made thin film platinum RTDs that are inexpensive, reliable, rugged, and suitable for use in transient facilities. The conclusions from this investigation, as discussed in chapter 6, are summarized as follows:

1. The construction techniques produced RTDs with the desired characteristics. By closely following the construction techniques as detailed in chapter 3, an experienced investigator can produce reliable, rugged, hand-made RTDs.

2. The self-heating tests showed that ohmic heating is practically zero up to an excitation voltage of about 1 V and that the effects can be accounted for in the final calculations for values up to 2 V. For excitation values greater than 2 V the internal heat generation increases rapidly and burnout usually occurs before an excitation of 4 V is reached.

3. Static calibration tests confirmed the expected linearity of the platinum film resistance as a function of temperature and the average temperature coefficient of resistance was found to be 0.019 K^{-1}. The expected conclusion that the sensitivity of the RTD could be significantly increased with a bridge circuit was also evidenced. Furthermore, a correlation of the RTD sensitivities showed an increasing linear trend with film resistance.

4. From the dynamic calibration tests it was found that excitation values between 5–10 V were adequate for obtaining accurate thermal product values. Excitation values greater than 10 V also produced adequate results, but there was a high rate of failure due to RTD burnout. The average value of the thermal product was determined to be 0.2 $J/cm^2/K/s^{1/2}$.

5. The final shock tube tests proved that hand-made thin film RTDs can be used to accurately measure heat transfer rates in transient facilities.

Recommendations

A complete study of transient thin film heat transfer gauges will require more testing. Several recommendations for further testing are:

1. It is recommended that other techniques of depositing the thin platinum film on the substrate are investigated and the results compared with the hand-made films. Sputtering techniques and vacuum deposition are two methods that could be used.

2. The shock tube tests should be repeated using several RTDs under several different flow velocities to confirm the reliability of the gauges. The ruggedness of the films should also be tested by subjecting the RTD to flows with much higher Mach numbers.

3. The effective thickness of the thin films should be investigated. A new experimental method for determining the film thickness is given by Buttsworth in ref. 18.

4. Methods for reducing the noise in the experimental data should also be considered.

REFERENCES

1. Bechwith, T., "Thermoresistive Elements", Mechanical Measurements, Addison-Wesley, Reading, 1995, pp. 668-673.
2. Holman, J. P., "Basic Electrical Measurements and Sensing Devices", Experimental Methods for Engineers, 5th edition, McGraw-Hill, 1989, pp. 113-121. Mechanical Measurements, Addison-Wesley, Reading, 1995, pp. 668-673.
3. Carslaw H. S. and Jaeger J. C., "The Infinite and Semi-infinite Solid", Conduction of Heat in Solids, 2nd edition, Clarendon Press, 1989, pp. 75-76.
4. Schultz, D.L. and Jones, T.V., "Heat-Transfer Measurements in Short-Duration Hypersonic Facilities," AGARDograph No. 163, February 1973, Department of Engineering Science, University of Oxford, Great Britain.
5. Cook W. J. and Felderman E. J., "Reduction of Data from Thin-Film Heat-Transfer Gages: A Concise Numerical Technique", AIAA Journal, Vol. 4, No. 3, 1966, pg. 561.
6. MACOR: Machinable Glass Ceramic, Corning Glass Works, Corning, New York.
7. Ligrani, P.M., Camci, C. and Grady, M.S., "Thin Film Heat Transfer Gage Construction and Measurement Details," TM33, Nov. 1982, von Karman Institute for Fluid Dynamics, Rhode Saint Genese, Belgium.
8. Olivier, H., Vetter, M., and Gronig, H., "Measurements on Models for Hypersonic Real Gas Conditions", New Trends in Instrumentation for Hypersonic Research, 1993, pp. 471-480.
9. Chung, K. M., "Shock Tube Calibration of a Fast-Response Pressure Transducer", M.S.A.E., The University of Texas at Arlington (UTA), 1989.
10. John, James E. A., "Normal Shock Waves", Gas Dynamics, 2nd edition, Allyn and Bacon, 1984, pp. 63-87.
11. Anderson, John D., "Shock Tube Relations", Modern Compressible Flow, 2nd edition, McGraw-Hill, 1990, pg. 237.
12. Bertin, John J., "Stagnation-Region Flowfield", Hypersonic Aerothermodynamics, American Institute of Aeronautics and Astronautics, 1994, pp. 249-255.